Full Paper

Applied Organometallic Chemistry

Received: 18 December 2007 Revised: 20 March 2008 Accepted: 20 March 2008 Published online in Wiley Interscience:

(www.interscience.com) DOI 10.1002/aoc.1412

Synthesis and structural investigations on R_2Sn(IV)-D-aldonic acid complexes (R = methyl; butyl). Their effect on a new toxicity test organism, *Liza saliens* (Osteichthyes, Mugilidae): a histological study

Nuccio Bertazzi[a], Girolamo Casella[a], Paolo D'Agati[b], Tiziana Fiore[a], Caterina Mansueto[b], Valentina Mansueto[b], Claudia Pellerito[a], Lorenzo Pellerito[a]* and Michelangelo Scopelliti[a]

Eight R_2Sn(IV)-D-aldonate complexes [(R = Me, Bu; D-aldonate = D-galactonate^{2-} (Galn), D-Gluconate^{2-} (Glun), D-Gulonate^{2-} (Guln), D-Ribonate^{2-} (Ribn)], five of which are new derivatives, have been synthesized and structurally characterized both in solid and solution state by IR, ^{119}Sn Mössbauer and ^{1}H, ^{13}C, ^{119}Sn NMR spectroscopies, showing that ligands act as dianonic chelating agents. In solution phase, NMR data suggest that the bidentate chelation is attained by the O1 carboxylate and the vicinal O2 alkoxide atoms, which can be dynamically extended to a third binding site (O4) competing with O2. In Me_2Sn(IV)-D-gluconate complex the occurrence of a self-association process leading to a dimeric species was also observed. Histopathological studies on different organs of *Liza saliens* showed that the dibutyltin(IV)-D-aldonate complexes, although preserving the defense immunity system, exhibit a specific toxicity on some target cells and organs. The toxicity of such complexes has been compared with respect to the effects of a previous study with tributyltin(IV) chloride solutions.

Keywords: organotin(IV); carbohydrates; toxicity; *Liza saliens*; histopathology; Mössbauer; FT-IR; NMR

Introduction

The interactions between organotin(IV) moieties and carbohydrates and their derivatives have been the subject of several investigations concerning the regioselective properties of diorganotin(IV) moieties (especially dibutyltin) in carbohydrates synthetic chemistry[1] and their biological activity.[2,3] In water solution, the formation of metal or organometallic ion complexes with sugar moieties depends on the competition between the ligand hydroxyl groups and solvent molecules and it has been observed that the coordination properties of simple sugars are dependent on the steric arrangement of hydroxyl groups as well as on the solution pH.[2] The presence of an anchoring group (e.g. carboxylate, phosphate, amine, thiol) makes the sugar molecule more effective towards the formation of stable complexes in water.[2] As far as diorganotin(IV) moieties with acidic carbohydrates derivatives are concerned, it has been shown that the sugar often acts as dianionic chelating ligand, via carboxylate and suitable alkoxidic groups, even at low pH.[4–6]

Aldonic acids are a class of acidic carbohydrates derivatives used in industrial,[7,8] medical[9,10] and cosmetic[11–13] applications or as intermediates in organic synthesis.[14–16] An IR and Mössbauer solid-state study of a hydrated dibutyltin(IV) gluconate compound (Bu_2SnGlun · H_2O) and a potentiometric and ^{13}C NMR solution investigation of Me_2SnGlun have been already reported.[6] Furthermore, recently an experimental ^{1}H, ^{13}C, ^{119}Sn NMR and ^{119}Sn NMR DFT solution study of the Me_2SnRibn complex has been reported.[17] In this paper we present a structural study on the complexes, five of which are new derivatives, obtained between some of these ligands (Fig. 1) and R_2Sn(IV) moieties (R = Me, Bu). Histology has provided a rapid method to detect effects of the pollutants in various fish tissues and organs.[18–21] In this respect these diorganotin(IV) derivatives have been tested on *Liza saliens* juveniles, a species already usefully employed to evaluate chemical toxicity,[22] and their biological activity has been compared with the effects of tributyltin(IV) chloride[22] using light microscope and histopathological techniques. In fact, in aquatic systems, tributyltin(IV) chloride is considered to be the most toxic organotin moiety, 10–100 times more toxic than dibutyltin(IV) moiety and its toxicity decrease with progressive de-alkylation to di- and mono-organotins.[23,24] However, according to a previous study,[25] dibutyltin(IV) proved to be a more powerful immunotoxin

* *Correspondence to: Lorenzo Pellerito, Dipartimento di Chimica Inorganica e Analitica 'Stanislao Cannizzaro', Università degli Studi di Palermo, Viale delle Scienze, Parco d'Orleans II, Edificio 17, 90128 Palermo, Italy. E-mail: bioinorg@unipa.it*

a *Dipartimento di Chimica Inorganica e Analitica 'Stanislao Cannizzaro', Università degli Studi di Palermo, Viale delle Scienze, Parco d'Orleans II, Edificio 17, 90128 Palermo, Italy*

b *Dipartimento Biologia Animale,'Giuseppe Reverberi', Università degli Studi di Palermo, Via Archirafi 18, 90123 Palermo, Italy*

than tributyltin(IV), and this suggested a need for the reassessment of the potential toxicity of dibutyltin(IV) to aquatic organisms.

Experimental

Materials and methods

For all the complexes, the analytical data indicated a 1 : 1 R_2Sn:L stoichiometric ratio with the aldonic acid acting as dianionic ligand. The complexes were analyzed, in our laboratory, for C, H contents using a Vario EL III CHNS elemental analyzer (Elementar Analysensysteme GmbH, Hanau, Germany). The tin content was analyzed gravimetrically as SnO_2 according to Neumann.[26] Discrepancies in the tin content are probably imputable to the behavior observed for other organotin(IV)-carbohydrates derivatives which, after the thermal decomposition, may give final products others than SnO_2, such as mixtures of SnO_2, SnO and even Sn.[27]

All complexes were synthesized from R_2SnO, freshly prepared by hydrolysis of the parent R_2SnCl_2 (Fluka, Buchs, Switzerland), (R = Me, Bu). The ligands were purchased as lactones, namely: D-galactono-1,4-lactone (γ-Galn), D-glucono-1,5-lactone (δ-Glun), D-gulono-1,4-lactone (γ-Guln) and D-ribono-1,4-lactone (γ-Ribn) (Sigma, St Louis, MO, USA; Fluka, Buchs, Switzerland) and were used without further purification according to the following procedures.

Me_2SnL (**1**–**4**): 1 mmol of *L* (*L* = γ-Galn, δ-Glun, γ-Guln, γ-Ribn) was dissolved in 20 ml of a 1 : 1 (v/v) water–ethanol (95%) mixture and kept refluxing for 1 h to open the lactonic ring. Solid Me_2SnO (1mmol) was then added, obtaining for **1, 2** and **4** a clear solution which was stirred for 2 h. After cooling, the solvent was removed in a rotovapor device, obtaining a white solid which was recrystallized from hot methanol and dried under vacuum over P_4O_{10}. For **3**, after the addition of solid Me_2SnO, a white precipitate was formed which was filtered, washed with cold methanol and dried under vacuum over P_4O_{10}. [Anal.: found (calcd) %, $Me_2SnGaln$ (**1**) ($C_8H_{16}O_7Sn$), C, 28.23 (28.02); H, 4.65 (4.71); Sn, 32.71 (34.62); $Me_2SnGlun$ (**2**), C, 27.05 (28.02); H, 4.46 (4.71); Sn, 33.50 (34.62); $Me_2SnGuln$ (**3**), C, 27.64 (28.02); H, 4.41 (4.71); Sn, 32.95 (34.62); $Me_2SnRibn$ (**4**) ($C_7H_{14}O_6Sn$), C, 26.48 (26.87); H, 4.67 (4.51); Sn, 39.38 (37.91).]

Bu_2SnL (**5**–**8**): 1 mmol of *L* (*L* = γ-Galn, δ-Glun, γ-Guln, γ-Ribn) was dissolved in 20 ml of a 1 : 1 (v/v) water–ethanol (95%) mixture and kept refluxing for 1 h to open the lactonic ring. Solid Bu_2SnO (1 mmol) was then added, obtaining a clear solution after *ca* 40 min and was left under stirring for 4 h. The water was removed by adding benzene to the water–ethanol mixture and azeotropic distillation. The volume of solvent was reduced to about 10 ml. On cooling, a white precipitate was obtained which was recrystallized from hot acetone, washed with chloroform and dried under vacuum over P_4O_{10}. [Anal.: found (calc)%, $Bu_2SnGaln$ (**5**) ($C_{14}H_{28}O_7Sn$), C, 38.91 (39.37); H, 6.12 (6.62); Sn, 27.91 (27.80); $Bu_2SnGlun$ (**6**) ($C_{14}H_{28}O_7Sn$), C, 39.46 (39.37); H, 6.46 (6.62); Sn, 28.02 (27.80); $Bu_2SnGuln$ (**7**) ($C_{14}H_{28}O_7Sn$), C, 39.36 (39.37); H, 6.59 (6.62); Sn, 28.10 (27.80); $Bu_2SnRibn$ (**8**) ($C_{13}H_{26}O_6Sn$); C, 38.86 (39.32); H, 6.65 (6.61); Sn, 26.88 (29.89).]

Spectroscopic data

FTIR spectra were recorded, both as nujol and hexachlorobutadiene mulls, on a Perkin-Elmer model Spectrum ONE FT-IR, in CsI windows, with eight averaged scans at 4 cm^{-1} resolution. The ^{119}Sn Mössbauer spectra were recorded with a model 269 TAKES (Ponteranica, Italy) controller and the following MWE (München Wissenschaftilche Elektronik, Gmbh, Starnberg, Germany) apparatus: MR250 driving unit, FG2 digital function generator and MA250 velocity transducer, moving at linear velocity and constant acceleration in a triangular waveform. A cryostat (NDR-1673-MB, Cryo Instruments, USA) with an ITC-2 Oxford Instrument temperature controller was used to maintain the absorber samples (absorber thickness, [^{119}Sn] = 0.50–0.60 mg cm^{-2}) at the investigated temperature (77.3 ± 0.1 K). The multichannel calibration was performed with an α-^{57}Fe foil (thickness 4 μm, Ritverc GmbH, Russian Federation) at RT using a ^{57}Co/Rh source (10 mCi, Ritverc GmbH), while the zero point of the Doppler velocity scale was determined at room temperature through the absorption spectrum of natural $CaSnO_3$ ([^{119}Sn] = 0.50 mg cm^{-2}) as source. Each collected spectrum had an average count of 5×10^5 per channel.

The pH determination of the NMR samples was performed only for the D_2O solutions by a glass electrode with a CRIMSON pH-meter mod. CriMSO2000 at 298 K. The corresponding pD values given in Table 3 were obtained by the following equation: pD = pH + 0.41.[28]

^{119}Sn{^{1}H} NMR experiments were carried out at 298 K on a Bruker ARX 300 MHz (7.04 T) spectrometer at 111.92 MHz both in D_2O and DMSO-d_6 solutions with a spectral width of 400 ppm. One-dimensional ^{1}H and ^{13}C{^{1}H} and two-dimensional ^{1}H-COSY, ^{1}H-NOESY, (^{1}H-^{13}C)-HSQC, (^{1}H-^{13}C)-HMBC NMR experiments were carried out in D_2O solution on Bruker Avance II DMX 400 MHz (9.40 T) spectrometer at 400.15 MHz (^{1}H) and 100.63 MHz (^{13}C) with a spectral width of 8 and 200 ppm, respectively. ^{1}H-NOESY were acquired with different mixing times, ranging from 0.1 to 0.7 s. One-dimensional ^{1}H proton spectra in D_2O at different temperatures were also acquired for (**1**) and they were calibrated on the water signal according to $\delta_{HDO}(T) = 5.060-(0.0122\cdot T)+(2.11\times10^{-5})\cdot T^2$, where T = temperature in °C.[29] The (^{1}H-^{13}C)-HSQC, (^{1}H-^{13}C)-HMBC spectra for (**1**) and (**2**), used for the signal assignments, are reported as Supplementary Information.

For ^{119}Sn{^{1}H} NMR spectra, in both solvents, the tetramethyltin(IV) was employed as external reference (^{119}Sn, δ = 0.00 ppm). ^{1}H and ^{13}C resonances were calibrated on tetramethyl silane as external reference (^{1}H, δ = 0.00 ppm; ^{13}C, δ = 00.0 ppm). ^{119}Sn{^{1}H} and ^{13}C{^{1}H} spectra were acquired with broadband proton power-gated decoupling. For all nuclei, positive chemical shift had higher frequencies than the reference. ^{13}C{^{1}H} line widths (LW) in the text are considered as line width at half height. Concen-

Table 1. Infrared assignments of (ν_{COO}) for coordinated carboxylate groups and ($\nu_{C=O}$) lactones carbonyl frequencies

Compound	Assignments			
	$\nu_{C=O}$	$\nu_{a(COO)}$	$\nu_{s(COO)}$	$\Delta\nu_{(COO)}$
γ-Galn	1790 vs	–	–	–
$Me_2SnGaln$ (**1**)	–	1614 vs	1377 m	242
$Bu_2SnGaln$ (**5**)	–	1582 s	1471 mw	111
γ-Glun	1728 vs	–	–	–
$Me_2SnGlun$ (**2**)	–	1602 vs	1412 mw	190
$Bu_2SnGlun$ (**6**)	–	1579 s	1414 w,b	165
γ-Guln	1781 vs	–	–	–
$Me_2SnGuln$ (**3**)	–	1611 w	1401 m	210
$Bu_2SnGuln$ (**7**)	–	1600 vs	1419 mw	181
γ-Ribn	1781 vs	–	–	–
$Me_2SnRibn$ (**4**)	–	1642 vs	1363 m	279
$Bu_2SnRibn$ (**8**)	–	1570 s	1420 mw	150

Table 2. Mössbauer data, estimated C–Sn–C angles and idealized proposed geometries of the complexes[a]

Compound	Mössbaeur data[a] $\delta_1\delta_2$ (mm s^{-1})	$\lvert\Delta_{exp}\rvert_1\lvert\Delta_{exp}\rvert_2$ (mm s^{-1})	Δ_{calc}[c] (mm s^{-1})	$\Gamma_1\Gamma_2$ (mm s^{-1})	∠(C–Sn–C) ±13°	Geometry[b]
1	1.31	3.96	4.02	1.13	161°	Oh1
2	1.35	4.03	4.02 or 4.16	1.02	165°	Oh1 or Oh2
3	1.19	3.55	−3.20	1.16	134°	Tbp2
4	1.32	3.91	4.02	1.01	155°	Oh1
5	1.36	3.62	−3.20	1.04	146°	Tbp2
6	1.16	2.69	2.90	1.02	120°	Tbp1
	1.32	3.24	−3.20	1.02	127°	Tbp2
7	1.25	3.00	2.90	1.04	120°	Tbp1
	1.37	3.84	4.16	1.07	155°	Oh2
8	1.25	3.11	2.90 or −3.20	1.12	123°	Tbp1 or Tbp2

[a] Experimental Mössbauer parameters measured at liquid nitrogen temperature; isomer shift, $\delta \pm 0.02$, with respect to room temperature $Ca^{119}SnO_3$; nuclear quadrupole splitting, $|\Delta_{exp}| \pm 0.03$.

[b] The proposed idealize structures are reported in Fig. 2.

[c] The partial quadrupole splitting values (mm s^{-1}) employed were: $\{Me, Bu\}_{Oh} = -1.03$[32]; $\{COO^-_{un}\}_{Oh} = -0.11$ (calculated from $\{COO^-_{un}\}_{Tet}$[32]); $\{COO^-_{br}\}_{Oh} = 0.083$ (calculated from $\{COO^-_{un}\}_{Tba}$[33]) $\{ROH\}_{Oh} = 0.16$[4]; $\{RO^-\}_{Oh} = -0.32$ (calculated from $\{RO^-\}_{Tba}$[35]); $\{Me, Bu\}_{Tbe} = -1.13$[33]; $\{COO^-_{br}\}_{Tba} = 0.075$[33]; $\{COO^-_{br}\}_{Tbe} = 0.29$ (calculated from $\{COO^-_{br}\}_{Tba}$[33]); $\{RO^-\}_{Tba} = -0.29$[35]; $\{RO^-\}_{Tbe} = -0.19$ (calculated from $\{RO^-\}_{Tba}$[35]).

trations of γ-galn and δ-glun D_2O solutions were *ca* 0.06 M while for (**1**) and (**2**) the D_2O and DMSO-d_6 solutions were *ca* 0.07 M. The spectral data were determined after 24 h to allow the systems to equilibrate. In the solution-state discussion the oxygen atoms reported without the proton symbol are intended as alkoxidic ones.

Biological material

Liza saliens, Risso, 1810 (Mugilidae, Osteichthyes) juveniles, ranging from 20 to 30 mm in body length, were caught from the coast of Sferracavallo (Palermo, Sicily) from July until November. This mugilidae lives in the coastal waters in contact with sediments and therefore it is heavily exposed to environmental pollution. The juveniles were raised in eight cylindrical fibreglass aquaria, 30 cm in diameter and 30 cm in height, containing 10 L of Millipore-Filtered Sea Water (MFSW) or MFSW with added chemicals. The MFSW was continuously aerated and changed every day. The oxygen levels were kept in the 5.8–9.8 mg l^{-1} range while pH range was continuously monitored and kept between 7.23 and 8.25. The MFSW temperature was kept at 19 ± 2 °C and cycles of 16 h of light and 8 h of darkness were performed during the experiments. The animals were nourished every day with *Artemia salina* (SELC, Artemia systems, BAAS-Rode, Belgium). A total of 160 fish were divided equally as follows:

(i) Control groups: (1) reared in tanks with MFSW; (2) reared in tanks with 0.07% dimethyl sulfoxide (DMSO)/MFSW solution; (3) reared in tanks with 10^{-5} M solution of the ligands in MFSW; (4) reared in tanks with 10^{-7} M solution of the ligands in MFSW.

(ii) Dimethyltin(IV)-D-aldonate derivatives groups: (5) reared in tanks with dimethyltin(IV)-D-aldonate derivatives 10^{-5} M in MFSW solution; (6) reared in tanks with dimethyltin(IV)-D-aldonate derivatives 10^{-7} M in MFSW solution.

(iii) Dibutyltin(IV)-D-aldonate derivatives groups: (7) reared in tanks with dibutyltin(IV)-D-aldonate derivatives 10^{-5} M in 0.07% DMSO/MFSW solution; (8) reared in tanks with dibutyltin(IV)-D-aldonate derivatives 10^{-7} M in 0.07% DMSO/MFSW solution.

Histology

The experiment was carried out over 20 days. Five fish were sampled from each tank, anaesthetized with 0.01% MS-222 (tricaine methanesulfonate; Sigma) and fixed in Bouin's liquid, pH 7.2 for 5 days at 25 °C. The fish were dehydrated through a graded series of ethanol infiltrated and embedded in paraplast. The histological specimens were cut into 5 µm transverse sections on a rotary microtome, stained with Gomori's trichrome; nuclei were stained black, cytoplasm/muscle red and collagen/connective tissue green. Light microscope observations were carried out by using a Leitz Diaplan microscope and pictures were obtained using Kodak Tmax films.

Results and Discussion

Solid state study

Infrared spectra

In Table 1 are given the ν_{COO} infrared absorption bands of coordinated carboxylate groups as well as the $\nu_{(C=O)}$ for the starting lactones (ν_{OH} and $\nu_{a(C-Sn-C)}$ and $\nu_{s(C-Sn-C)}$ infrared absorptions are given as Supplementary Information, Table S1). The lactonic $\nu_{(C=O)}$ absorptions in the 1790–1720 cm^{-1} range are no longer observed in the complexes due to the opening of the lactonic ring. The $\nu_{a(COO)}$ stretchings for the complexes are in the 1640–1570 cm^{-1} range as usually observed for carboxylates groups bound to organotin(IV) moieties[6] and exclude the occurrence of free COOH. The corresponding $\nu_{s(OCO)}$ are localized in the 1470–1360 cm^{-1} range. The estimated $\Delta\nu = \nu_{a(OCO)} - \nu_{s(OCO)}$ values would indicate[30] a unidentate carboxylate coordination mode in the case of **1, 3** and **4**, and the occurrence of bridging caboxylate groups for **5**–**8**; for **2** the $\Delta\nu$ value does not allow a clear distinction between the two binding modes.[30]

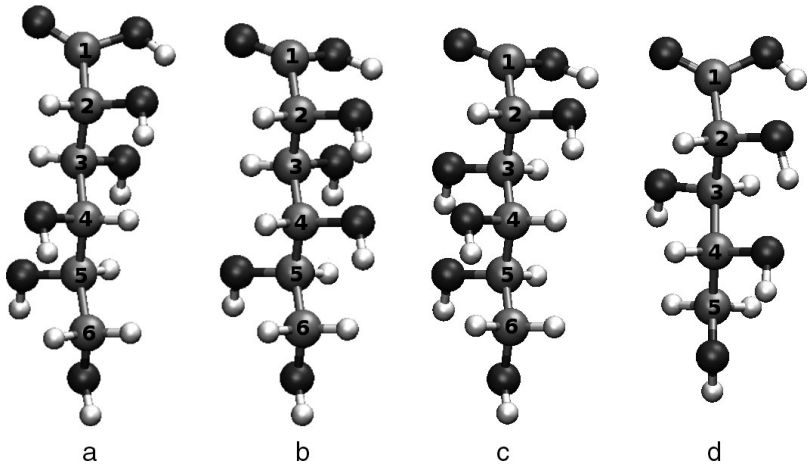

Figure 1. Three dimensional representation of (a) D-galactonic acid, (b) D-gluconic acid, (c) D-gulonic acid and (d) D-ribonic acid, and numbering of the carbon atoms.

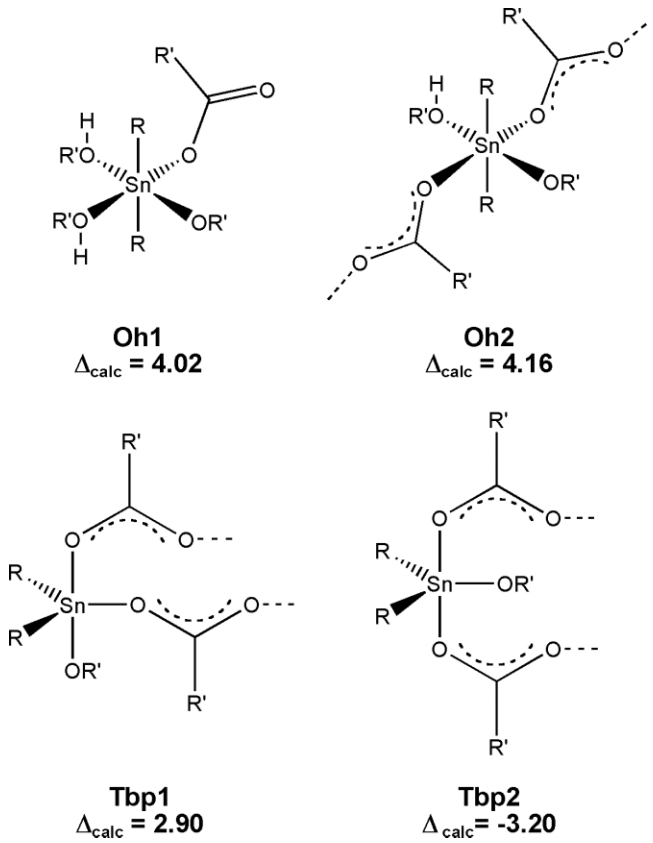

Figure 2. Proposed idealized structures for the complexes according to the point charge formalism (R = Me, Bu; OR′ = alkoxidic oxygen; R′OH = alcoholic oxygen).

^{119}*Sn Mössbauer spectra*

The Mössbauer data are shown in Table 2. The compounds have fairly large nuclear quadrupole splitting ($|\Delta_{exp}|$) values; the calculation based on the simple point charge treatment of Sham and Bancroft,[31] which assumes the splitting to be due solely to the disposition of the Sn–C bonds, gives C–Sn–C bond angles ranging from 120 to 165°.

Table 2 also gives the quadrupole splitting values calculated (Δcalc) using the point charge model formalism[31–34] for the idealized spatial arrangements of Fig. 2. For the dimethyltin(IV) compounds **1, 2** and **4**, the six-coordinated structure **Oh1** appears the most suitable; however, **Oh2** remains a possibility for (**2**) in consideration of its borderline infrared $\Delta\nu$ value (Table 1). For compound (**3**) Mössbauer data point to a **Tbp2** configuration which implies a polymeric arrangement with bridging carboxylate groups and it appears possible that, in consideration also of its poor solubility, the infrared $\Delta\nu = 210\ cm^{-1}$ value may not actually reflect an unidentate carboxylate behavior.[30] For the dibutyltin(IV) derivatives **5**–**8**, Mössbauer data are in agreement with a **Tbp** local geometry. The best fit of spectral data for **6** has been obtained assuming the presence of two different **Tbp** tin centres. A similar two-sites fit has been reported for the mentioned Bu_2Sn(IV)Glun · H_2O.[6] We note that the two products are not identical since they differ for one water molecule in their formula, which might well be responsible for the different spectral parameters. Evidence of two sites has been obtained also in the case of **7**, where one tin centre is better described by an **Oh2** geometry. All the proposed structures for dibutyltin(IV) compounds consider the occurrence of intermolecular interaction.

Solution-state investigation by NMR spectroscopy

Solution-state investigations were carried out for the soluble dimethyltin(IV) derivatives (**1**) and (**2**) by ^{1}H, ^{13}C and ^{119}Sn NMR spectroscopy. For complex (**4**) the NMR solution-state investigation has been recently reported and it has been shown that ^{1}H NOE, ^{119}Sn resonances and ^{13}C line-width analysis give useful information about the coordinating sites and the occurrence of self-association processes.[17] Complexes **3** and **5**–**8** were not investigated because of their very low solubility in common NMR solvents.

^{119}*Sn{*^{1}*H} NMR spectra*

In D_2O **1** and **2** show a broad signal at −110 ppm (LW = 1200 Hz) and at −120 ppm (LW = 1350 Hz), respectively, characteristic of penta-coordinated dimethyltin(IV) species.[36,37] In DMSO-d_6 **1** presents a single resonance at −96 ppm (LW = 650 Hz) while **2** shows two signals at −107 ppm (LW = 140 Hz) and at −298 ppm (LW = 350 Hz). In DMSO-d_6 the signals for both complexes appear

Table 3. $^{13}C\{^1H\}$ and ^1H chemical shifts (ppm) of the lactones, free acids and complexes at 298 K

Compound	C1[a]	C2	C3	C4	C5	C6	CH_3	H2	H3	H4	H5	H6	H6′	CH_3
GalnA pD = 3.7	180.2	73.3	73.9	71.9	72.6	66.0	–	4.55	4.09	3.68	n.a	3.73	3.72	–
Me_2SnGaln (**1**) pD = 4.6	182.6 (35)	72.1 (18)	71.5 (6)	69.4 (18)	69.7 (8)	62.6 (7)	2.7 (33)	4.47	3.97	3.70	3.95	3.71	3.68	0.77
$\Delta\delta$	2.4	−1.2	−2.4	−2.5	−2.9	−3.4	–	−0.08	−0.12	0.02	0.01	−0.02	−0.04	–
GlunA pD = 3.0	178.5	74.9	73.7	73.3	74.1	65.3	–	4.41	4.08	3.73	3.72	3.77	3.60	–
Me_2SnGlun(**2**) pD = 4.5	181.4[b] (–)	75.9 (16)	70.2 (8)	73.5 (12)	71.2 (3)	63.0 (4)	4.2 (48)	4.36	4.10	3.87	3.73	3.80	3.64	0.81
$\Delta\delta$	2.9	1.0	−3.5	0.2	−2.9	−2.3	–	−0.05	0.02	0.14	0.01	0.03	0.04	–

[a] Line width in Hz in parentheses.
[b] Signal assigned from the ($^1H-^{13}C$)-HMBC spectrum.

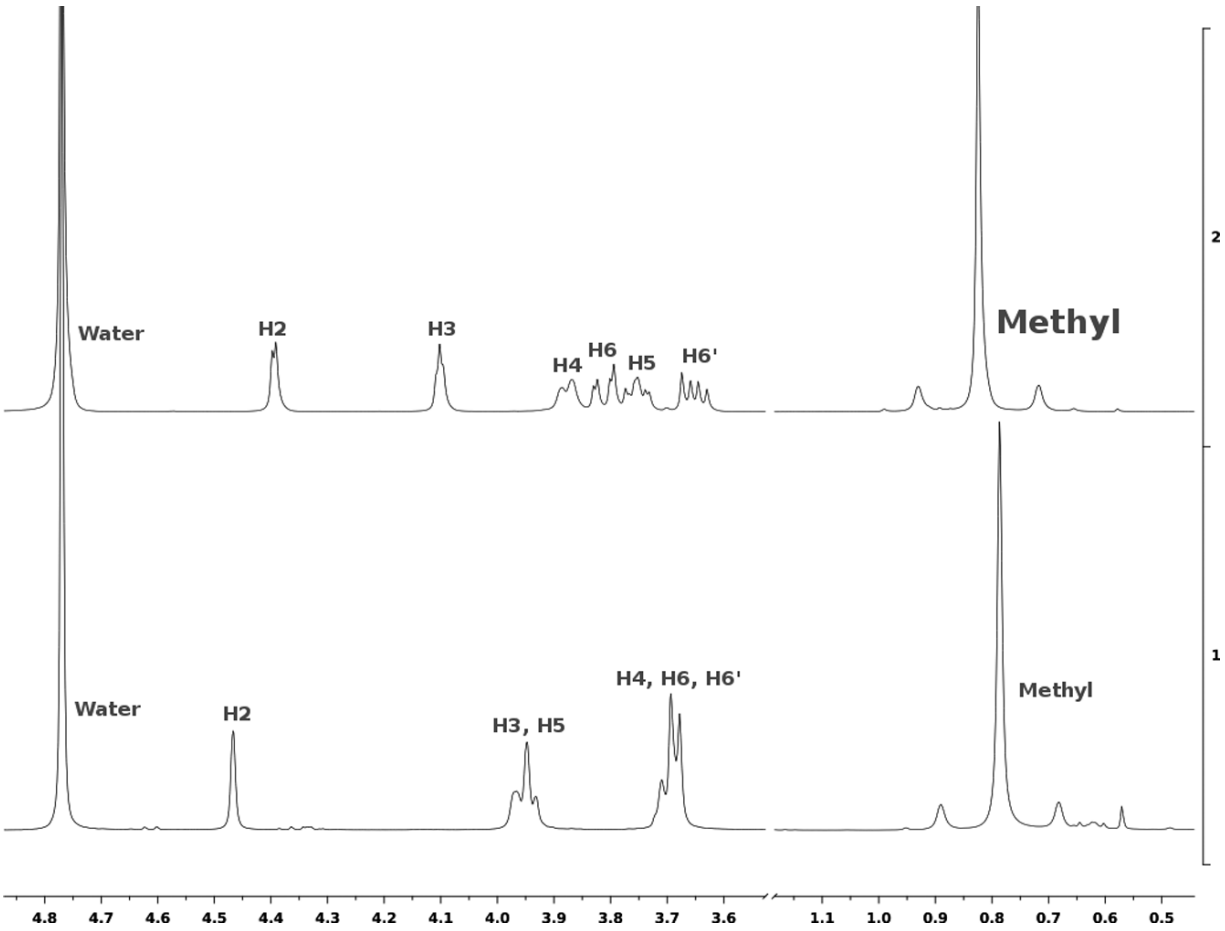

Figure 3. Selected regions of the ^1H spectra (values in ppm) for Me_2SnGaln (**1**) and Me_2SnGlun (**2**), showing the broadening of the ligand signals.

sharper than those in D_2O showing a systematic increase of ^{119}Sn δ in accordance with what has been observed for similar systems.[4,17] This behavior was expected on the basis of the different coordinating properties of the two solvents and indicates the occurrence of tin–solvent exchange equilibria. For **2**, the appearance of the second resonance in DMSO-d_6 (at −298 ppm) attributable to a hexa-coordinated dimethyltin(IV) species[36,37] also points to the occurrence of self-association processes, as already advanced in the case of **4**.[17]

^1H and $^{13}C\{^1H\}$ NMR spectra

The D_2O solution-state ^1H and $^{13}C\{^1H\}$ δs for **1**, **2** and for related ligands are given in Table 3 (^1H and $^{13}C\{^1H\}$ δs of the corresponding aldonic forms are given as Supplementary Information; Table S2). In the case of the ligands, the signals of both the lactonic and the free acidic forms are observed. In particular, for the equilibrated δ-glucono lactone solution, the ^1H and $^{13}C\{^1H\}$ spectra showed the simultaneous occurrence of the free acidic, the δ and γ forms (Table S2 in Supplementary Information). The presence in the **1** and **2** spectra of a unique pattern corresponding to the ligands acidic form of the ligands is indicative of aldonate derivatives formation.

In the ^1H spectra for **1** and **2**, the signals appear broad, indicating the probable occurrence of exchanging species in solution (Fig. 3). As a matter of this, for **1**, improvement in the signals resolution is observed by increasing the temperature and the shape of

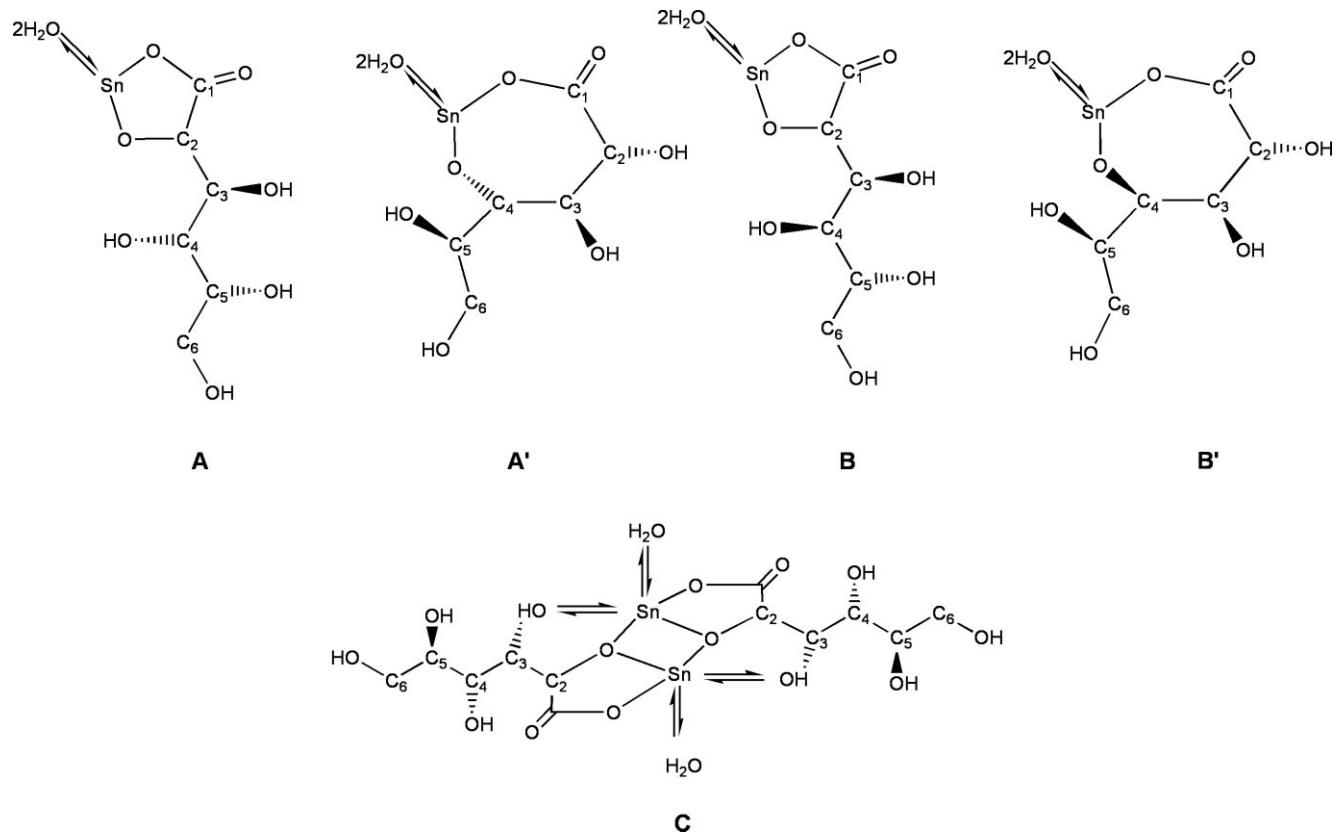

Figure 4. Proposed configuration in solution for **1** and **2**. (A) and (B): monomeric forms for **1** and **2**, respectively, with the ligands acting as dianionic chelating ones via O2; (A′) and (B′): monomeric forms for **1** and **2**, respectively, with the ligands acting as dianionic chelating ones via O4; (C) dimeric structure for **2** showing the Sn–OH(3) interaction. The double arrows indicate the occurrence of exchanging water in the tin coordination sphere as well as, in the case of C, the competition between water and OH(3) for the tin center. Methyl groups have been omitted.

the resolved CH_3Sn satellites at higher temperatures does not correspond to the typical pattern of $^2J[^{117}Sn,^1H]$ and $^2J[^{119}Sn,^1H]$ couplings, strongly supporting the occurrence of different species in solution (see Fig. S5 in Supplementary Information).

In the ^{1}H-NOESY spectra (see Figs S6 and S7 in Supplementary Information), spatial correlations H2–CH_3, H4–CH_3 for both compounds and an additional H3–CH_3 cross-peak only for **2** are observed. The H2–CH_3 dipolar interaction is in agreement with the coordination of O2 to the tin atom. Moreover, the H4–CH_3 dipole–dipole couplings support the view that OH4, as an alcoxidic species, is also involved in the tin coordination, competing with O2 probably via proton-catalyzed cleavage of the Sn–O bonds[5] [Fig. 4(A,A′ and B,B′)]. The observed H3–CH_3 dipolar interaction for **2** is indicative of an Sn–OH(3) interaction due to the formation of a dimeric species [Fig. 4(C)]. H2–H3 and H2–H4 dipolar interactions for the two compounds are also observed in the ^{1}H-NOESY spectra, which can be explained by admitting a suitable arrangement of this protons in the ring resulting from the Sn–O4 interaction [Fig. 4(A′, B′)].

In the ^{1}H spectra the magnitudes of the observed $^2J[^{117,119}Sn,^1H]$ satellites flanking the CH_3Sn proton signals (Fig. 3) are 84.2 ± 5.0 and 85.2 ± 5.0 Hz for **1** and **2,** and by using the above values in the Lockhart–Manders relation,[38] the C–Sn–C angles calculated for the compounds are: (136 ± 7)° and (138 ± 7)°, respectively. The uncertainty in the values arises from the large broadening of the corresponding satellites at 298 K. The estimated C–Sn–C values indicate a skew-octahedral local tin geometry attributable either to the monomeric forms of **1** and **2**, which consider the presence of water molecules in the tin coordination sphere, as well as the dimeric form of **2**, where a competitive Sn–OH(3) and Sn–H_2O interaction cannot be excluded [Fig. 4(C)].

In the CH_3Sn region the spectra of **1** and **2** show some low-intensity signals corresponding to the typical CH_3Sn pattern, at 0.57 and 0.58 ppm, flanked by the $^2J[^{117,119}Sn,^1H]$ whose measured integrated intensities are 3 and 1%, respectively. For both systems the $^2J[^{117,119}Sn,^1H]$ values are *ca* 70 Hz giving estimated C–Sn–C angles of *ca* 120°, which do not match any of the proposed geometries. These signals are imputed to side products, possibly hydrolyzed species, and have not been further investigated.

In the $^{13}C\{^1H\}$ spectra, the broadening of some ^{13}C signals (Table 3), not observed in the corresponding ligands spectra, confirmed the occurrence of dynamic processes in the NMR time scale: besides the broadening of the C1 and CH_3Sn signals occurring in the spectra of both compounds, the broadening of the C2, C4 and the C2, C3 and C4 signals has been also observed for **1** and **2**, respectively (Figs S8 and S9 in Supplementary Information; the measured LW are reported in Table 3). The signal broadening of C2 indicates that also in solution the ligands act as dianionic chelating agents via the deprotonated O2 [Fig. 4(A, B)]. Moreover, the C4 broadening in **1** and **2**, is similar to that observed for C2 (Table 3) and confirms that both O4 and O2 are interacting with the tin atom. For **2**, the small C3 broadening together with the previously discussed H3-CH_3 ^{1}H-NOESY dipole coupling give further evidence of the dimer formation via inter-molecular Sn–OH(3) interaction. Finally, the large broadening of the carbon CH_3 signals

Table 4. Effects of dibutyltin(IV)-derivatives, 10^{-5} M solutions, on selected target organs of *Liza Saliens*

Organ	Compound 5	6	7	8
Gills	Detached secondary *lamellae* epithelial cells; red cells deprived of hemoglobin; picnotic nuclei	Fused erythrocytes; picnotic nuclei; hemoglobin around the nuclei; degranulating cells near gills; edema in epithelium of secondary *lamellae*	Detached secondary *lamellae* epithelial cells; red cells deprived of hemoglobin; picnotic nuclei	Compacted, shape-altered erythrocytes of primary and secondary *lamellae*; picnotic nuclei; swollen epithelium in secondary *lamellae*
Heart	Relaxed musculature; detached muscle bands; altered erythrocytes; pigment around the nuclei; fine granulation in heart cells	Relaxed musculature; detached muscle bands; altered erythrocytes; pigment around the nuclei; fine granulation in heart cells	Relaxed musculature; detached muscle bands; altered erythrocytes; pigment around the nuclei	Relaxed musculature; detached muscle bands; altered erythrocytes; pigment around the nuclei; fine granulation in heart cells
Liver	Detached hepatocyte cords; clear cytoplasm; compacted, irregular shape erythrocytes with reduced pigment; dilated sinusoid	Detached hepatocyte cords; clear cytoplasm; compacted, irregular shape erythrocytes with reduced pigment; dilated sinusoid	Detached hepatocyte cords; clear cytoplasm; compacted, irregular shape erythrocytes with reduced pigment; dilated sinusoid	Detached hepatocyte cords; clear cytoplasm; compacted, irregular shape erythrocytes with reduced pigment; dilated sinusoid
Kidney	Irregular outline of cells surrounding the tubules; fused and accumulated erythrocytes; fragmented chromatin in renal tubule cells; melanomacrophage aggregate	Irregular outline of cells surrounding the tubules; fused and accumulated erythrocytes; fragmented chromatin in renal tubule cells	Irregular outline of cells surrounding the tubules; fused and accumulated erythrocytes; fragmented chromatin in renal tubule cells	Irregular outline of cells surrounding the tubules; fused and accumulated erythrocytes; anomalous nephrons, lymphocytes, erythrocytes
Thymus	Overdeveloped cortical part; fused red cells	Fused red cells	Overdeveloped cortical part; fused red cells	Irregular outline cells; heavily colored plasm; fused and hemolised erythrocytes
Pancreas	As in the control	Altered, pigment-deprived erythrocytes; destroyed islet of Langerhans; pink stained fine granulation adherent to pancreas	As in the control	Altered, pigment-deprived erythrocytes; destroyed islet of Langerhans; pink stained fine granulation adherent to pancreas
Spleen	As in the control	Anomalous erythrocytes; prevalence of lymphocytes along the connective septa	As in the control	Fused erythrocytes; hemoglobin around the nucleus; broken red cells; fine powder outside the nucleus
Muscles	As in the control	Lightly detached fibres; fused or shape-altered erythrocytes	As in the control	Lightly detached fibres; fused or shape-altered erythrocytes
Intestine	Fused erythrocytes even at the bottom of villi	As the control	As in the control	As in the control
Gonad	Less colored than control; degranulating cells	Less colored than control; degranulating cells	Less colored than control; degranulating cells	Slightly separated and degranulating cells near gonads

also points to the occurrence of several equilibria involving the tin atom attributable to tin-ligands and tin–solvent exchange.

Biological investigation

The *in vivo* experiments and histological studies carried on juveniles of *Liza saliens* showed that only the dibutyltin(IV)-derivatives solutions at concentration of 10^{-5} M produce alterations in liver, heart, kidney, spleen, pancreas, gills and on erythrocytes. The results are summarized in Table 4; selected images are available as Supplementary Information. The controls appear as described in the literature.[39] Compounds **6** and **8** are more toxic than **5** and **7**, the ligands and the dimethyltin(IV) complexes causing no effect on the fish juveniles. The immuno-defense system was not attacked by tested compounds, and activation of degranulating cells was noted around the gills and gonad, degranulation (and active substances release) being the characteristic acute response in tissues exposed to noxious agents. Such a response has been found to be similar in mammalians and salmonides.[40] In *Liza saliens*, it seems to be present a general response after chemical treatment. As far as the erythrocytes were concerned, morphological alterations were observed in some cases.

It is noteworthy that in many cells of renal tubule there is a clear fragmented of chromatin, and the cells lose their junctions. The absence of normal cohesion is probably due to the fact that cells are destroyed by the chemical. The hystopatological study also demonstrated that the DBT-derivatives exhibit a specific toxicity on some target organs: **6** and **8** heavily modify the pancreatic structure by destroying the erythrocytes with a consequent hemoglobin pouring (observed as a fine granular pink pigment outside the organ). Such induced alterations, however, appear less severe than those observed for TBTCl on the same species;[22] alterations in eyes, gills, muscles, liver, intestine, pancreas and heart were already observed at 10^{-7} M TBTCl, along with thymus atrophy, spleen reduction and alteration of head and kidney. Muscle fibres

appeared normal after treatment: the treated fishes moved as the controls, and the histological study showed that only for **6** and **8** the muscle fibres were slightly detached.

Conclusions

In the studied dimethyltin(IV)- and dibutyltin(IV)-D-aldonate derivatives the ligands act as dianionic chelating agents via the carboxylate and a suitable deprotonated alcoholic group. The solid-state investigation showed that the carboxylate may behave as monodentate as well as bridging bidentate but could not indicate which alkoxidic group is acting as the second coordinating site. The NMR investigation in aqueous solution, performed on the soluble $Me_2SnGaln$ (**1**) and $Me_2SnGlun$ (**2**), showed that O2 is the second binding site which, in the case of the monomeric species, competes with O4. At the investigated concentrations it has been observed that **2** undergoes self-association. It is noteworthy that the occurrence of dimerization in water is inferred from the $^{13}C\{^1H\}$ spectrum while the $^{119}Sn\{^1H\}$ NMR measurements did not give evidence of this.

The histological study carried out on *Liza saliens* selected target organs showed that the dibutyltin(IV)-D-aldonate derivatives at 10^{-5} M concentration exhibit a specific toxicity on the selected target organs which proved to be lower than that of triorganotin(IV) chloride, since organ alterations appeared reduced and the immuno-defense system preserved. The toxicity observed for the present dibutyltin(IV) D-ribonate and D-gluconate is higher than that of D-galactonate and D-gulonate.

Supplementary Material

Supplementary electronic material for this paper is available in Wiley InterScience at: http://www.interscience.wiley.com/jpages/1099-0739/suppmat/

Acknowledgments

Financial support by the Ministero dell'Istruzione, dell'Università e della Ricerca (MIUR, CIP 2004059078_003), Roma and the Università di Palermo (ORPA06K3RK) is gratefully acknowledged. NMR experimental data obtained with the Bruker Avance II DMX 400 MHz spectrometer were provided by Centro Grandi Apparecchiature, UniNetLab, Università di Palermo funded by POR Sicilia 2000-2006, Misura 3.15 Quota Regionale.

References

[1] T. B. Griendly, *Adv. Carbohydr. Chem.* **1998**, *53*, 17.
[2] B. Gyurcsik, L. Nagy, *Coord. Chem. Rev.* **2000**, *203*, 81.
[3] L. Pellerito, L. Nagy, *Coord. Chem. Rev.* **2002**, *224*, 111.
[4] N. Bertazzi, G. Bruschetta, G. Casella, L. Pellerito, E. Rotondo, M. Scopelliti, *Appl. Organomet. Chem.* **2003**, *17*, 932.
[5] N. Bertazzi, G. Casella, F. Ferrante, L. Pellerito, A. Rotondo, E. Rotondo *Dalton T.* **2007**, 1440.
[6] A. Szorcsik, L. Nagy, B. Gyurcsik, G. Vankó, R. Krämer, A. Vértes, T. Yamaguchi, K. Yoshida, *J. Radioanal. Nucl. Ch.* **2004**, *260*, 459.
[7] K. Larsson, O. Samuelson, *J. Chromatogr. A* **1977**, *134*, 195.
[8] B. W. Chun, B. Dair, P. J. Macuch, D. Wiebe, C. Porteneuve, A. Jeknavorian, *Appl. Biochem. Biotechnol.* **2006**, *131*, 645.
[9] R. J. Klauser, W. Raake, E. Meinetsberger, P. Zeiller, *J. Pharmac. Exp. Ther.* **1991**, *259*, 8.
[10] W. Raake, R. J. Klauser, H. Elling, P. Zeiller, E. Meinetsberger, *Semin. Thromb. Hemost.* **1994**, *20*, 176.
[11] R. J. Yu, E. J. Van Scott, U. S. Patent 5,583,156, August **1997**.
[12] R. J. Yu, E. J. Van Scott, U. S. Patent 5,656,666, August **1997**.
[13] A. Khaiat, J. C. Bernard, Fr. Demande, 2,707,647 (Cl. C078K4/10), **1995**.
[14] K. L. Bath, C. S. Yih, M. M. Joullié, *Heterocycles* **1985**, *23*, 691.
[15] L. Salmon, E. Prost, C. Merienne, R. Hardre, G. Morgant, *Carbohydr. Res.* **2001**, *335*, 195.
[16] M. Godskesen, I. Lundt, B. Winchester, *Bioorg. Med. Chem.* **1996**, *4*, 1857.
[17] A. Bagno, N. Bertazzi, G. Casella, L. Pellerito, G. Saielli, I. D. Sciacca, *J. Phys. Org. Chem.* **2006**, *19*, 874.
[18] P. Visoottiviseth, T. Thamamaruitkun, S. Sahaphong, S. Riengrojpitak, M. Kruatrachue, *Appl. Organomet. Chem.* **1999**, *13*, 749.
[19] D. Y. Wang, B. Q. Huang, *Zoological Studies* **1999**, *38*, 189.
[20] M. Pacheco, M. A. Santos, *Ecotox. Environ. Safety* **2002**, *53*, 332.
[21] I. S. Rabitto, J. R. M. Alves Costa, H. C. Silva de Assis, E. Pelletier, F. M. Akaishi, A. Anjos, M. A. F. Randi, C. A. Oliveira Ribeiro, *Ecotox. Environ. Safety* **2005**, *60*, 147.
[22] P. D'Agati, C. Mansueto, V. Mansueto, M. V. Cangialosi, T. Fiore, C. Pellerito, L. Pellerito, *Appl. Organomet. Chem.* **2006**, *20*, 357.
[23] J. A. J. Thompson, M. G. Sheffer, R. C. Pierce, Y. K. Chau, J. J. Cooney, W. R. Cullen, R. J. Maguire, *Organotin Compounds in the Aquatic Environmental. Scientific Criteria for Assessing their Effects on Environmental Quality*. National Research Council Canada Publication No. NRCC 22494, **1985**.
[24] P. W. Wester, J. H. Canton, *Comp. Biochem. Physiol.* **1991**, *100C*, 115.
[25] K. O'Halloran, J. T. Ahokas, P. F. A. Wright, *Aquat. Toxicol.* **1998**, *40*, 141.
[26] W. P. Neumann, *The Organic Chemistry of Tin* (Ed.: W. P Neumann). Interscience: London, **1970**.
[27] J. D. Donaldson, S. G. Grimes, L. Pellerito, M. A. Girasolo, P. J. Smith, A. Cambria, M. Famà, *Polyhedron* **1987**, *6*, 383.
[28] A. K. Convington, M. Paabo, R. A. Robinson, R. G. Bates, *Anal. Chem.* **1968**, *40*, 700.
[29] H. E. Gottlieb, V. Kotlyar, A. Nudelman, *J. Org. Chem.* **1997**, *62*, 7512.
[30] G. B. Deacon, R. J. Phillips, *Coord. Chem. Rev.* **1980**, *33*, 227.
[31] T. K. Sham, G. M. Bancroft. *Inorg. Chem.* **1975**, *14*, 2281.
[32] G. M. Bancroft, R. H. Platt, *Adv. Inorg. Chem. Rad.* **1972**, *15*, 59.
[33] G. M. Bancroft, V. G. Kumar Das, T. K. Sham, *J. Chem. Soc. Dalton Trans.* **1976**, 643.
[34] R. Barbieri, A. Silvestri, F. Huber, C. D. Hager, *Can. J. Spectrosc.* **1981**, *26*, 194.
[35] L. Korecz, A. A. Sahiger, K. Burger, A. Tzschach, K. Jurkschat, *Inorg. Chim. Acta* **1982**, *58*, 243.
[36] B. Wrackmeyer, *Annu. Rep. NMR Spectrosc.* **1985**, *16*, 73.
[37] B. Wrackmeyer, *Annu. Rep. NMR Spectrosc.* **1999**, *38*, 203.
[38] T. P. Lockhart, W. F. Manders, *Inorg. Chem.* **1986**, *25*, 892.
[39] H. Takashi, *An Atlas of Fish Histology: Normal and Pathological Features*. Stuttgart Publications: New York, **1982**.
[40] O. B. Reite, *Fish. Shellfish. Immun.* **1997**, *7*, 567.